Optical phase retrieval by phase-space tomography and fractional-order Fourier transforms

D. F. McAlister, M. Beck,* L. Clarke, A. Mayer,† and M. G. Raymer

Department of Physics and Chemical Physics Institute, University of Oregon, Eugene, Oregon 97403

Received December 19, 1994

Phase-space tomography is experimentally demonstrated for the determination of the spatially varying amplitude and phase of a quasi-monochromatic optical field by measurements of intensity only. Both fully and partially coherent sources are characterized. The method, which makes use of the fractional-order Fourier transform, also yields the Wigner distribution of the field and works in one or two dimensions.

Phase retrieval is the determination of the transverse phase structure of an optical field.[1] Often interference with a reference field (i.e., holography) is used for this purpose.[2] Recently we proposed and analyzed a concept for phase retrieval in which the phase structure is obtained purely from intensity measurements, using no reference fields.[3] The method can be applied in the cases of fully or partially coherent sources and is based on phase-space tomography in which the Wigner distribution function is reconstructed from intensity measurements.[4] An advantage of the tomographic method is that the data analysis requires no deconvolution and is noniterative, in contrast to most established phase-retrieval techniques. Other noninterferometric and self-interferometric methods have been developed, although such methods are not applicable for the case of partial coherence with arbitrary correlation function.[5–7] This Letter presents to our knowledge the first experimental demonstrations of the new method.[8]

Define a quasi-monochromatic wave field $E(x)$, where the amplitude E is the (scalar and dimensionless) electric-field strength and x is the transverse position. We consider only fields dependent on a single transverse coordinate, although the method generally uses two such variables.[3] In the case of partial coherence, where an ensemble of stochastic fields is under consideration, a useful characterization is provided by the two-point field correlation function, also called the mutual intensity, equal to

$$\Gamma(x,x') = \langle E(x)E^*(x')\rangle, \tag{1}$$

where the angle brackets indicate an average over the set of realizations of the function $E(x)$ and $\int \Gamma(x,x)\,dx = 1$.

The wave field to be reconstructed, $E(x,0)$, is located in the $z = 0$ plane (see Fig. 1) and has a (longitudinal) propagation constant denoted k. The field propagates through a cylindrical lens of focal length f located at $z = d$ and oriented to refract in the x dimension. The field, $E(x,D,d,f)$, in a plane $z = D > d$ is determined by a Fresnel integral,[3] for which it is convenient to define a curvature radius $R = R_0 + d$, with $1/R_0 = 1/(D-d) - 1/f$, and an effective propagation length $L = (D-d)(1 + d/R_0)$. The measurable intensity distributions $I(x,D,d,f) = \langle |E(x,D,d,f)|^2\rangle$ are normalized to unity when integrated in x.

Define a scaled transverse position $\chi \equiv x/x_0$ and a scaled transverse wave number $\eta \equiv k_x x_0$, where x_0 is a characteristic length. The wave field to be reconstructed may also be represented in terms of its Wigner quasi-distribution function defined in the χ, η phase space as[9]

$$W(\chi,\eta) = \frac{1}{\pi}\int_{-\infty}^{\infty}\langle E(\chi+\chi')E^*(\chi-\chi')\rangle \times \exp(-i2\chi'\eta)\,d\chi'. \tag{2}$$

Although $W(\chi,\eta)$ can be negative, its integrated (marginal) distributions are positive and are directly measurable. Defining a new pair of rotated phase-space variables according to $\chi_\theta = \chi\cos\theta + \eta\sin\theta$ and $\eta_\theta = \eta\cos\theta - \chi\sin\theta$, we can find a set of marginal distributions, $P_\theta(\chi_\theta)$, for these variables. $P_\theta(\chi_\theta)$ is given by a phase-space projection integral through the Wigner distribution along parallel lines of constant χ_θ. These marginal distributions can be written as[3]

$$P_\theta(\chi_\theta) = \langle |E_\theta(\chi_\theta)|^2\rangle, \tag{3}$$

where $E_\theta(\chi_\theta)$ is a transformed field function. For $\theta = \pi/2$ this field is proportional to the Fourier transform of $E(\chi)$; for $\theta = 0$ it is equal to $E(\chi)$. For θ between 0 and $\pi/2$ the field in some sense interpolates between $E(\chi)$ and its Fourier transform and thus has been referred to as the fractional-order Fourier transform.[10]

As proved in Ref. 3, $E_\theta(\chi_\theta)$ in Eq. (3) is identical in form to the Fresnel integral that determines $E(x,D,d,f)$. The equivalence between the two is established by the following correspondences. Rescale the transverse coordinate according to $\chi = -\chi_\theta(L\csc\theta/kx_0^2)$ and identify $\cot\theta = -kx_0^2/R$ to determine the phase-space rotation angle θ. We control this angle by varying R, which depends on d, f, and D. With these $E_\theta(\chi_\theta)$ is identical to $E(x,D,d,f)$ to within an unimportant x-dependent phase factor. Measuring the intensity $I(x,D,d,f)$ for a particular value of

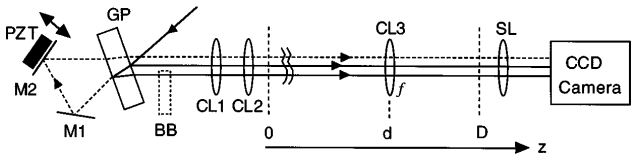

Fig. 1. Experimental setup.

0146-9592/95/101181-03$6.00/0

R thus determines $P_\theta(\chi_\theta)$ for the corresponding angle, θ, according to

$$P_\theta(\chi_\theta) = I[-\chi_\theta(L \csc \theta/kx_0), D, d, f\,]. \qquad (4)$$

Our method is to measure a sufficiently large set of these distributions for different values of θ to allow the Wigner function to be reconstructed tomographically by means of the inverse Radon transform.[11,12] Then Eq. (2) can be inverted to yield the field correlation function $\Gamma(\chi, \chi') = \langle E(\chi)E^*(\chi')\rangle$.

To demonstrate this method we have reconstructed two wave fields, one of which has full spatial coherence, the other exhibiting only partial coherence. The output of a He–Ne laser is spatially filtered in a single-mode optical fiber. Then, using the two surface reflections from a glass plate (GP), we create two spatially separated, nearly parallel beams (see Fig. 1). A constant relative phase is maintained between these beams so that together they represent a field with full spatial coherence. To create a field depending only on a single transverse dimension, we expand the two beams in the vertical dimension, using cylindrical lenses CL1 and CL2. The wave field then consists of highly elliptical beams, which near the vertical center depend only on the horizontal transverse dimension x. This field, located in the $z = 0$ plane, is the field that is reconstructed.

We allow the field to propagate and pass through an $f = 20$ cm focal-length cylindrical lens, CL3, located at $z = d$. This cylindrical lens is oriented 90° with respect to both CL1 and CL2 so as to affect only the horizontal transverse dimension. The desired intensities, located in the $z = D$ plane, are imaged with a magnification of approximately 3 onto a CCD camera by a spherical lens, SL. The filtered backprojection algorithm that we use for tomographic reconstruction requires marginal distributions $P_\theta(\chi_\theta)$ for N equally spaced angles over the range $\theta = [-\pi/2, \pi/2)$. To achieve these phase-space rotation angles according to $\cot\theta = -kx_0^2/R$, we mount lenses CL3 and SL and the camera on an optical rail, allowing d and D to be varied. Here $k = 2\pi/632.8$ nm is the wave number of the light, and we chose $x_0 = 0.0006$ m. A total of $N = 32$ angles were used, for which it was sufficient to use values of D from 1.2 to 2.0 m and values of d from 0.8766 to 1.7524 m. For each combination of d and D, the intensity distribution $I(x, D, d, f)$ was digitized, normalized, and scaled to give the marginal distributions shown in Fig. 2(a). By performing the inverse Radon transform we reconstruct the Wigner function from which we obtain the field correlation function $\Gamma(\chi, \chi')$.

Figure 3(a) shows the magnitude squared of this function, $|\Gamma(\chi, \chi')|^2$. For the reasons mentioned above we expect this field to be coherent. In this case a single field contributes to the ensemble average in Eq. (1), allowing $\Gamma(\chi, \chi')$ to be factorized as $\Gamma(\chi, \chi') = E(\chi)E^*(\chi')$. The complex wave field, $E(\chi) = |E(\chi)|\exp\{i[\phi(x) + \delta_0]\}$, then provides complete characterization and can be determined to within an unphysical constant phase, δ_0, by fixing χ' to be a constant in $\Gamma(\chi, \chi')$.

The reconstructed field's intensity, $|E(\chi)|^2$, and phase structure, $\phi(\chi)$, are shown in Fig. 3(c). The phase structure is consistent with that expected from the experimental parameters. Note the discrete phase jump between the beams caused by their path-length difference. Examination of $|\Gamma(\chi, \chi')|^2$ explicitly

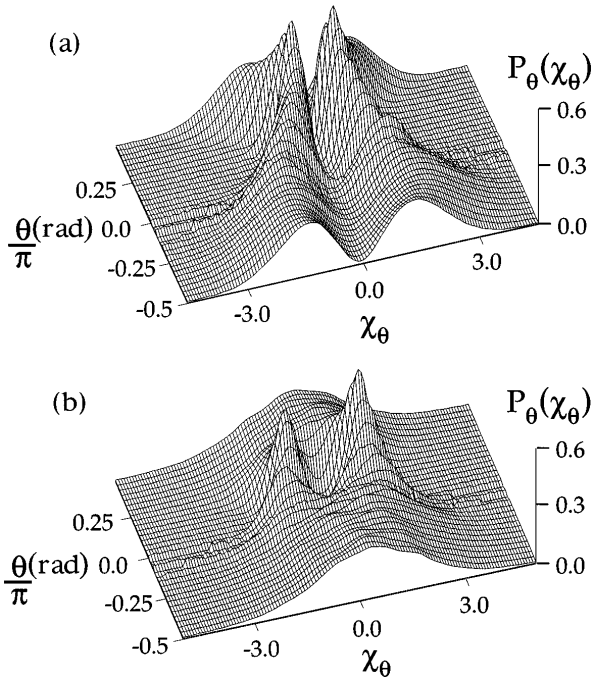

Fig. 2. Measured scaled intensity distributions for (a) the fully coherent field and (b) the partially coherent field.

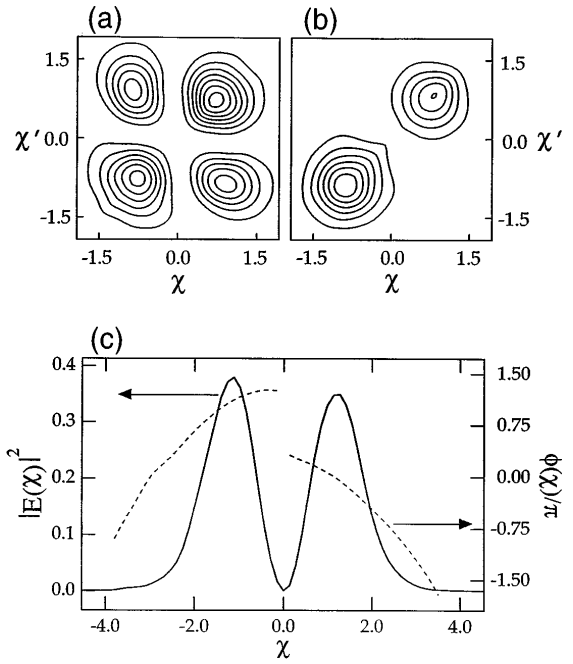

Fig. 3. Equal separation contours showing the magnitude squared of the reconstructed field correlation function, $|\Gamma(\chi, \chi')|^2$, for (a) the fully coherent field and (b) the partially coherent field. (c) The intensity profile (solid curve) and the phase structure (dashed curves) of the reconstructed complex wave field obtained in the fully coherent case. Where the intensity is near zero the phase is undefined and is not plotted.

demonstrates that each beam in the field is well correlated with itself ($+\chi$ is correlated to $+\chi'$ and $-\chi$ is correlated to $-\chi'$) and the two beams are well correlated with each other ($\pm\chi$ shows strong correlation with $\mp\chi'$).

The second field that we reconstructed was created by a third beam that initially passes through the glass plate and is recombined nearly parallel to the reflected beams by mirrors M1 and M2 (Fig. 1). A piezoelectric translator (PZT) is mounted on M2 and is driven to randomize the relative phase between this third beam and the reflected beams. Blocking the lower reflected beam (with beam block BB) then creates a field similar in intensity to the field reconstructed above, except that it is partially coherent.

Using the same parameters and positions described above, we obtained the normalized marginal distributions for this case as shown in Fig. 2(b). The relative phase between the beams is varied on a time scale that is much shorter than the camera integration time, so that the camera effectively conducts the ensemble average in Eq. (1). The effect of this is to wash out any interference between the two beams, causing the dark central fringe prevalent in Fig. 2(a) to disappear. Figure 3(b) shows the magnitude squared of the reconstructed field correlation function. In contrast to the field correlation function shown in Fig. 3(a), this consists of only two peaks. This indicates that, although each beam is correlated with itself, the randomized relative phase destroyed their previous correlation with each other.

The extent to which the field is coherent can be quantified in a fashion analogous to the purity of a quantum state described by a density matrix. Only when the trace $\mathrm{Tr}(\Gamma^2) = \int \Gamma^2(\chi, \chi')\,\mathrm{d}\chi\mathrm{d}\chi' = 1$ does Γ describe a fully coherent field, whereas for $\mathrm{Tr}(\Gamma^2) < 1$ the field is partially coherent. Only in the former case can Γ be factorized in terms of a single complex wave field. On the other hand, in the case of two well-separated beams with random relative phase, as is the case for the second reconstructed field, the result should be $\mathrm{Tr}(\Gamma^2) = 1/2$.

From the first field reconstructed we calculate $\mathrm{Tr}(\Gamma^2) = 0.85$, compared with the expected result of $\mathrm{Tr}(\Gamma^2) = 1$, and from the second field reconstructed we calculate $\mathrm{Tr}(\Gamma^2) = 0.45$, compared with the expected result of $\mathrm{Tr}(\Gamma^2) = 1/2$. Although in a strict sense the former result invalidates our previous factorization to obtain the complex wave field shown in Fig. 3(c), there are no physical reasons for this field not to be fully coherent. We searched for the source of these errors by numerically simulating various sets of intensity distributions and found the reconstruction method to be quite resilient to errors in the parameters f, d, and D and the magnification (effect of lens SL in Fig. 1), even for errors that are well above our estimated errors. A known source of error results from amplitude fringes that are due to interference of the coherent light in the CCD chip. Also, the camera has auto-gain-control circuitry and therefore is not completely linear in incident intensity. Based on this, we attribute the discrepancies in $\mathrm{Tr}(\Gamma^2)$ to errors in the measured intensity distributions.

In summary, we have successfully reconstructed optical wave fields along a single transverse dimension by using phase-space tomography. The reconstruction of fields with differing spatial coherence properties demonstrates the usefulness of this method over previous noninterferometric phase-retrieval techniques.

We thank A. Faridani for providing the numerical algorithm used for the tomography. This research was supported by the U.S. Army Research Office and the National Science Foundation. A. Mayer is a participant in the Research Experience for Undergraduates Program of the National Science Foundation, through a grant to the Chemical Physics Institute, University of Oregon.

*Present address, Department of Physics, Reed College, Portland, Oregon 97202.

†Present address, College of William and Mary, Williamsburg, Virginia 23187.

Noted added in proof: After our submission of this Letter, a similar experiment was reported.[13]

References

1. J. R. Fienup, Appl. Opt. **21,** 2758 (1982).
2. K. Creath, in *Progress in Optics XXVI,* E. Wolf, ed. (Elsevier, Amsterdam, 1988), p. 349.
3. M. G. Raymer, M. Beck, and D. F. McAlister, Phys. Rev. Lett. **72,** 1137 (1994); in *Quantum Optics VI,* D. F. Walls and J. D. Harvey, eds. (Springer-Verlag, Berlin, 1994), p. 245.
4. There are analogs of phase-space tomography for time-frequency-domain reconstructions [M. Beck, M. G. Raymer, I. A. Walmsley, and V. Wong, Opt. Lett. **18,** 2041 (1993)] as well as quantum-mechanical state reconstruction [D. T. Smithey, M. Beck, M. G. Raymer, and A. Faridani, Phys. Rev. Lett. **70,** 1244 (1993)].
5. N. Streibl, Opt. Commun. **49,** 6 (1984); K. Ichikawa, A. W. Lohmann, and M. Takeda, Appl. Opt. **27,** 3433 (1988).
6. D. Kohler and L. Mandel, J. Opt. Soc. Am. **63,** 126 (1972).
7. K.-H. Brenner and A. W. Lohmann, Opt. Commun. **42,** 310 (1982).
8. D. F. McAlister, M. Beck, and M. G. Raymer, presented at the Annual Meeting of the Optical Society of America, Dallas, Tex., October 2–7, 1994.
9. For a review see M. Hillery, R. F. O'Connel, M. O. Scully, and E. P. Wigner, Phys. Rep. **106,** 121 (1984); M. J. Bastiaans, J. Opt. Soc. Am. A **3,** 1227 (1986).
10. V. Namias, J. Inst. Math. Appl. **25,** 241 (1980); H. M. Ozaktas, B. Barshan, D. Mendlovic, and L. Onural, J. Opt. Soc. Am. A **11,** 547 (1994); A. W. Lohmann, J. Opt. Soc. Am. A **10,** 2181 (1993).
11. This reconstruction idea was first pointed out in a quantum context by J. Bertrand and P. Bertrand, Found. Phys. **17,** 397 (1987); see also P. Bertrand and J. Bertrand, Reck. Aerosp. **5,** 277 (1985) for time frequency.
12. G. T. Herman, *Image Reconstruction From Projections: The Fundamentals of Computerized Tomography* (Academic, New York, 1980), p. 279.
13. B. Eppich and N. Reng, presented at the Laser Beam Control, Diagnostics, and Standards Conference, San Jose, Calif., February 6–7, 1995.